Friction between Diamond Surfaces in the Presence of Small Third-Body Molecules

Martin D. Perry and Judith A. Harrison*

Department of Chemistry, U.S. Naval Academy, Annapolis, Maryland 21402-5026

Received: August 20, 1996; In Final Form: December 16, 1996[⊗]

Molecular dynamics simulations have been used to examine the friction between the hydrogen-terminated (111) faces of diamond with small hydrocarbon (third-body) molecules trapped between them. In general, the presence of the trapped third-body molecules reduced the friction between the diamond surfaces with the most pronounced reduction at high loads. The size and shape of the third-body molecule, as well as the alignment of atoms on opposing diamond surfaces, were found to be paramount in determining the magnitude of the friction. These results are compared to results from previous simulations that examined the effects of chemically bound hydrocarbons on the friction between diamond surfaces and to available experimental data.

I. Introduction

Friction can be defined as the force that opposes the motion of two bodies in sliding contact.[1,2] The natural outcomes of friction are usually heating of the contacting materials, plastic deformation, and wear. In engineering applications, the natural outcomes of friction can lead to catastrophic failure of equipment. These catastrophic failures might be avoided if the origins of friction were understood.

The advent of new technology, capable of investigating friction and wear on the atomic scale, has shifted the focus of the experimental examination of friction from the macroscopic to the microscopic scale.[3] Instrumentation that has been used to examine atomic-scale friction includes the atomic force microscope (AFM),[4−8] the surface force apparatus (SFA),[9,10] and the quartz crystal microbalance.[11,10] Advances in computer technology have allowed for complementary theoretical investigations of atomic-scale friction and wear.[13−26] Theoretical techniques that have been employed to examine the atomic-scale origins of friction include first-principles calculations[14,15] and molecular dynamics (MD) simulations.[16−26] In some cases, theory and experiment agree quite well. For example, the wearless atomic-scale friction of diamond has been investigated using both the AFM[6] and MD simulations.[20,23] The MD simulations demonstrated that the friction for sliding on the (100) face of diamond was approximately the same as it was for sliding on the (111) face of diamond, in agreement with experimentally obtained data.

Because of diamond's unique friction and wear properties,[27] there has been a large number of experimental[6,16,27−33] and theoretical[19−25] studies that have investigated the friction and wear of diamond and carbon films. In this work, small hydrocarbon molecules were trapped between two (111) crystal faces of diamond and the friction and wear investigated using MD simulations. These trapped molecules (sometimes referred to as third-body molecules) might model hydrocarbon contamination that was trapped between contacting diamond surfaces prior to a sliding experiment. Alternatively, these molecules might model hydrocarbon debris that formed when two diamond surfaces were in sliding contact.[33] In separate studies, three simple hydrocarbon molecules were trapped between the hydrogen-terminated (111) faces of two diamond surfaces and atomic-scale friction as a function of load investigated. Results are compared to previous work that examined the friction behavior of two (111) faces of diamond with hydrogen termination[20,22] and hydrocarbon termination[21] and to available experimental data.

II. Methods and Procedures

Example simulation starting configurations for all the third-body systems examined are depicted in Figure 1. These systems have hydrocarbon molecules trapped between the (1 × 1) hydrogen-terminated (111) faces of two diamond surfaces. The carbon portion of the diamond surfaces consists of first- and second-layer carbon atoms that are trigonally arranged. The vertices of these triangles are rotated 60° with respect to one another, thus forming a hexagon. (It is important to note that the hexagon is not planar; rather, it is similar to the chair conformation in cyclohexane.) The hexagon is centered over a fourth-layer carbon atom (large light-gray sphere), which is visible through "holes" in the surface layers. The hydrogen atoms that cover the diamond surfaces are bound to the first-layer carbon atoms. Each diamond surface is composed of 11 layers of carbon atoms and one layer of hydrogen atoms. Each layer contains 16 atoms. Periodic boundary conditions are applied in the plane of the interface to simulate an infinite interface.

The trapped, or third-body, molecules examined are methane (CH_4), ethane (C_2H_6), and isobutane ($(CH_3)_3CH$). These systems (the third-body molecules plus the two diamond surfaces) will be referred to as the methane, the ethane, and the isobutane systems, respectively. (Because similar hydrocarbon debris might form while sliding, we have referred to the methane system as the methane-debris system in previous publications.[25]) The region between the two diamond surfaces will be referred to as the interface. In the methane system, two molecules are trapped between the diamond surfaces per periodic unit. Similar results are obtained on test simulations with one methane molecule trapped at the interface. Because of the size of the calculation cell, only one molecule per periodic unit is trapped at the interface in the ethane and isobutane systems.

Newton's equations of motion are not integrated for the two outermost layers of the upper and lower surfaces (Figure 1). That is, because the outermost layers are held rigid, their relative position is used to define the interface separation and thus, the applied load. (The rigidity of the outermost layers in the direction perpendicular to the sliding direction, and in the sliding plane, resembles an AFM experiment rather than an SFA

* To whom correspondence should be addressed (jah@brass.nadn.navy.mil).

⊗ Abstract published in *Advance ACS Abstracts,* February 1, 1997.

S1089-5647(96)02561-8

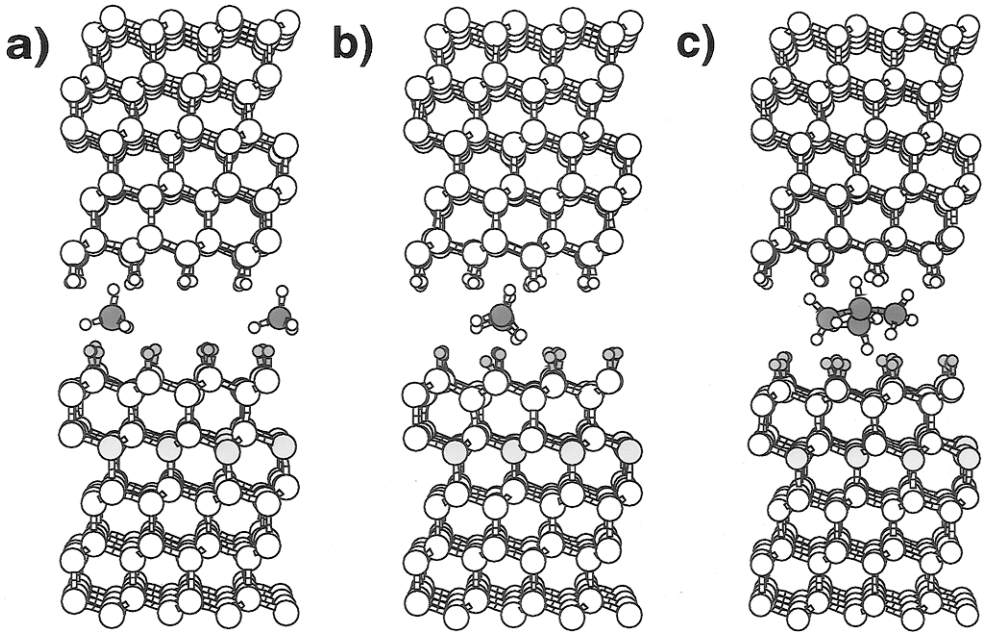

Figure 1. Initial configurations at low load for the diamond plus third-body molecule systems examined. These systems are composed of two diamond surfaces, viewed along the [$\bar{1}$10] direction, and two methane molecules (a), one ethane molecule (b), and one isobutane molecule (c). Large white and dark gray spheres represent carbon atoms of the diamond surfaces and the third-body molecules, respectively. Small gray spheres represent hydrogen atoms of the lower diamond surface. Hydrogen atoms of the upper diamond surface and the third-body molecules are both represented by small white spheres. Large light gray spheres represent fourth-layer carbon atoms of the lower diamond surface. During a sliding simulation, the rigid layers of the upper surface are slid from left to right in the figure.

experiment. Lateral movement in the direction perpendicular to sliding is allowed in an SFA experiment.) Nonrigid atoms dynamically evolve in time according to Newton's equations of motion, with the forces governing their motion derived from a reactive-empirical bond-order hydrocarbon potential.[34] These equations of motion are integrated using a third-order Nordsieck predictor-corrector[35] with a constant time step of 0.5 fs. The temperature of the system is maintained at 300 K by applying a thermostat to the middle five layers of each lattice.[36] (It should be noted, for temperatures around 300 K, the frictional force between the (111) faces of two diamond surfaces depends only slightly on temperature.[20] Therefore, no systematic attempt to examine the effects of temperature was made in this work.)

For all the sliding simulations, the upper surfaces in Figure 1 slide in the [11$\bar{2}$] crystallographic direction (from left to right in the figure) at a constant velocity of 100 m/s for 30.0 ps. (While the velocity dependence of the frictional force was not examined systematically in this work, previous simulations show that sliding an order of magnitude slower does not significantly affect the average frictional force.[20,23]) The normal load is increased by decreasing the separation between the rigid layers. During the course of a simulation, the frictional force (normal force) is taken to be the sum of the force in the sliding direction (normal to the interface) on the rigid-layer atoms. Forces are normalized by dividing by the number of rigid-layer atoms. Both the frictional force and the normal force oscillate during the course of simulation; therefore, the forces reported are averages over the entire simulation.

Because the relative lateral placement of the two opposing diamond surfaces affects the frictional force,[21] frictional force data (and normal force data) must be averaged over simulations whose starting configurations differ in lateral position of the upper surface.

Prior to the start of the sliding simulation, the third-body molecules are translationally and rotationally cold. The vibrational temperature of the molecules corresponds to approximately 300 K. The third-body molecules are placed between the two diamond surfaces and the systems are equilibrated using the thermostat. After the equilibration, the third-body molecules typically occupy a position between the two diamond surfaces that corresponds to a minimum energy structure. The position of the third-body molecule subsequent to the equilibration changes slightly depending on the relative placement of the opposing surfaces. In this work, no systematic attempt was made to examine the frictional force as a function of third-body-molecule starting orientation.

III. Results

A great deal of information pertaining to the atomic-scale friction of diamond has been provided by MD simulations.[19−25] Because diamond surfaces used in experiments are typically atomically rough, comparisons between simulations and experimental data are problematic. With this in mind, in previous MD simulations small hydrocarbon groups were chemisorbed to one of the (111) faces of diamond and friction was investigated.[21] Under certain conditions, the simulations showed that the hydrocarbon debris formed is consistent with experimentally observed debris.[24] Experiments have shown that this nascent debris has a profound effect on the friction between the diamond surfaces.[33] Thus, the friction of diamond in the presence of debris or third-body molecules should be examined.

A. Diamond Friction in the Presence of a Third Body. For all the systems examined, the average frictional force as a function of average normal load is shown in the lower panel of Figure 2. For comparison, frictional force data for the same system in the absence of the third-body molecules are also shown. Those data points that have lines extending above and below them represent frictional force values that are the average of values obtained from five independent starting configurations. These configurations differ in the relative position of the upper and lower diamond surfaces. One starting configuration corresponds to a situation where hydrogen atoms on opposing surfaces (small gray and small white spheres) lie along the same line in the sliding direction. (This starting configuration will

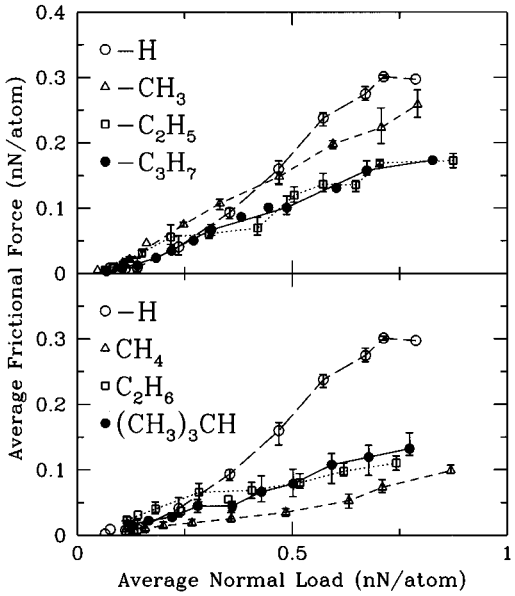

Figure 2. Average frictional force per rigid-layer atom as a function of average normal load per rigid-layer atom for sliding the upper diamond surface in the [11$\bar{2}$] crystallographic direction. Data for the methane (CH_4) system (open triangles), the ethane (C_2H_6) system (open squares), the isobutane ($(CH_3)_3CH$) system (filled circles), and diamond surfaces in the absence of third-body molecules (open circles) are shown in the lower panel. Data for the methyl-terminated ($-CH_3$ system (open triangles), the ethyl-terminated ($-C_2H_5$) system (open squares), the *n*-propyl-terminated ($-C_3H_7$) system (filled circles), and diamond surfaces in the absence of third-body molecules (open circles) are shown in the upper panel. Simulation conditions are described in the text. Lines have been drawn to aid the eye.

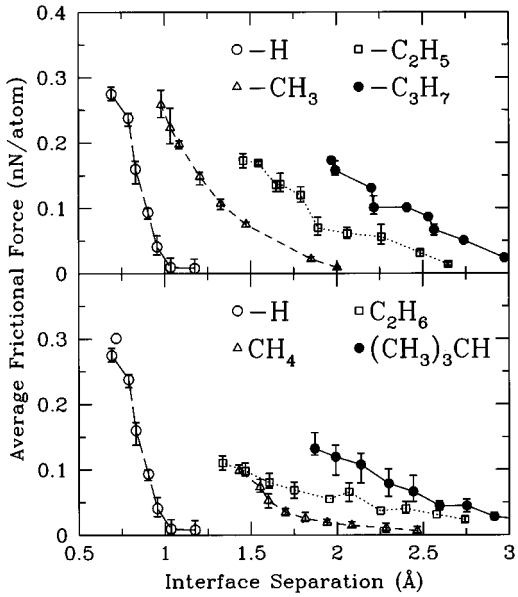

Figure 3. Average frictional force per rigid-layer atom as a function of interface separation for sliding the upper diamond surface in the [11$\bar{2}$] crystallographic direction. Data for the third-body and the chemisorbed systems are shown in the lower and upper panels, respectively. The symbols are the same as in Figure 2. Lines have been drawn to aid the eye.

be referred to as the "aligned" configuration.) Four other starting configurations are obtained by successive 0.313 Å translations of the upper surface in the [1$\bar{1}$0] crystallographic direction (see Figure 5). The repeat distance in the [1$\bar{1}$0] direction is 2.5 Å. However, the repeat distance is bisected by a mirror plane. Therefore, these five starting configurations span the repeat distance in the [1$\bar{1}$0] direction. The upper and lower lines drawn from these averaged points extend to the maximum and minimum values, respectively, of frictional force obtained from the five independent simulations. Thus, the lines represent the range of frictional force values obtained at a given load. Data points that do not have lines extending from them are the frictional force values obtained from one sliding simulation with aligned diamond surfaces.

In general, the frictional force increases as a function of normal load for all of these systems. However, as the load is increased the presence of all the third-body molecules markedly reduces the average frictional force. The methane system exhibits the lowest frictional force, while the ethane and isobutane systems have comparable frictional force values over the load range examined.

To explain this behavior, the origin of atomic-scale friction must be understood. Previous work has shown that atomic-scale friction is related to the dissipation of energy.[22] The larger the frictional force, the more energy dissipated. The amount of energy dissipated is quantified by plotting the vibrational energy between the interface carbon and hydrogen (C−H) layers of the diamond surface as the sliding progresses. For example, for hydrogen-terminated diamond in the absence of third-body molecules, vibrational excitation arises from the mechanical interaction of hydrogen atoms on opposing diamond surfaces during sliding. This interaction results in the vibrational excitation of the diamond, particularly the interface C−H layers. The amount of mechanical interaction, and thus vibrational excitation, increases as a function of load. Therefore, the friction increases as a function of load.

In general, the third-body molecules reduce friction by acting as a boundary layer between the two opposing diamond surfaces. This is apparent through examination of the average frictional force versus interface separation (i.e., the average distance between hydrogen atoms on opposing diamond surfaces) shown in Figure 3. The interfacial separation is always much larger when the third-body molecules are present compared to the separation in the absence of these molecules. As a result, the third-body molecules reduce the interaction of the hydrogen atoms on opposing diamond surfaces to an almost negligible amount. (Thus, the alignment of the surfaces is important only insofar as it affects the orientation of the third-body molecules.) In light of this, the interaction of the third-body molecules with the diamond surfaces while sliding must be responsible for most of the dissipated energy in these systems. Because the frictional force as a function of load is approximately the same for the ethane and the isobutane systems, approximately the same amount of energy must be dissipated during sliding in these two systems. In contrast, the lower frictional force in the methane system results in less energy dissipated while sliding. Thus, the methane molecules mechanically interact to a lesser extent with the diamond surfaces than the other third-body molecules while sliding.

The motion of the third-body molecules and the extent of their interactions with the diamond surfaces are dictated by their size and shape and the alignment of the diamond surfaces. Animated sequences of individual sliding simulations, or trajectories, are used to visualize the motion of the third-body molecules between the diamond surfaces during sliding. Taken together with plots of the frictional force as a function of unit cell distance (defined as sliding distance divided by the repeat distance in the sliding direction, or 4.357 Å), these sequences allow for full characterization of the motion of the third-body molecules and the extent of their interactions with the diamond surfaces.

The spherical shape and small size of the methane molecules cause the motion of the molecule to be similar regardless of

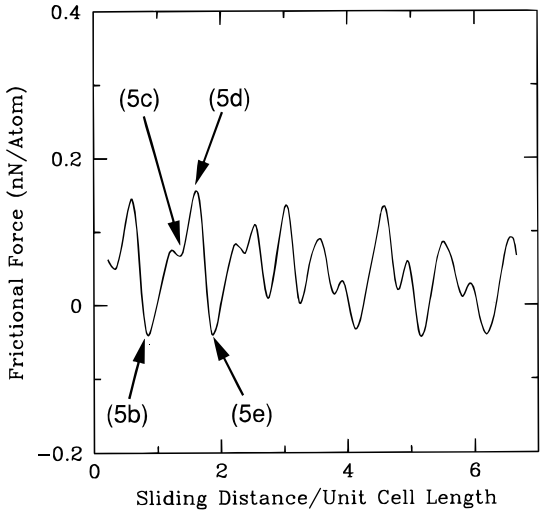

Figure 4. Frictional force as a function of sliding distance divided by unit cell length for a methane system simulation. (The sliding distance is divided by the unit cell length in the sliding direction, 4.357 Å, to yield a dimensionless quantity.) The average normal load and frictional force for this simulation are 0.65 and 0.046 nN/atom, respectively. These data correspond to the same methane system trajectory described in Figure 5 and the letters b, c, d, and e correspond to the configurations in that figure.

the load or diamond surface alignment. Therefore, the motion of the molecule is illustrated using data from one high-load (0.65 nN/atom) trajectory where the diamond surfaces are aligned. The frictional force as a function of unit cell distance and still images of this trajectory are shown in Figures 4 and 5a-e, respectively. The frictional force as a function of unit cell distance (referred to as a friction trace) is periodic. The periodic nature of the frictional force has been observed in both experiments[4,6] and previous simulations[20] and therefore is not surprising. The extrema in these data are correlated to configurations the methane molecules adopt relative to the diamond surfaces during sliding.

It is clear from an examination of the starting configuration (Figure 5a) that the methane molecules fit into the triangular spaces defined by the hydrogen atoms on the (111) crystal face of the diamond. In this configuration, both carbon atoms of the methane molecules are centered over the holes in the lower diamond surface. Sliding the rigid layers of the upper diamond surface at a constant velocity in the sliding direction causes the entire upper surface to move. The motion of the upper-surface hydrogen atoms has the effect of "sweeping" the methane molecules in the sliding direction. However, the methane molecules are not constrained to move in a straight line because they are not attached to the upper diamond surface. Because the lower surface is not being moved, the lower-surface hydrogen atoms remain in the same general area throughout the course of these simulations.

The motion of the upper surface causes the methane molecules to be swept to the positions shown in Figure 5b after 4.20 ps. Because the methane molecules are located over holes in the lower surface, they interact very little with the lower-surface hydrogen atoms (small gray spheres). As a result, this type of configuration corresponds to a minimum in the friction trace. The continued motion of the upper surface forces the methane molecules to interact with the hydrogen atoms directly in front of them in the sliding direction and gives rise to the increase in the frictional force (Figure 4). The methane

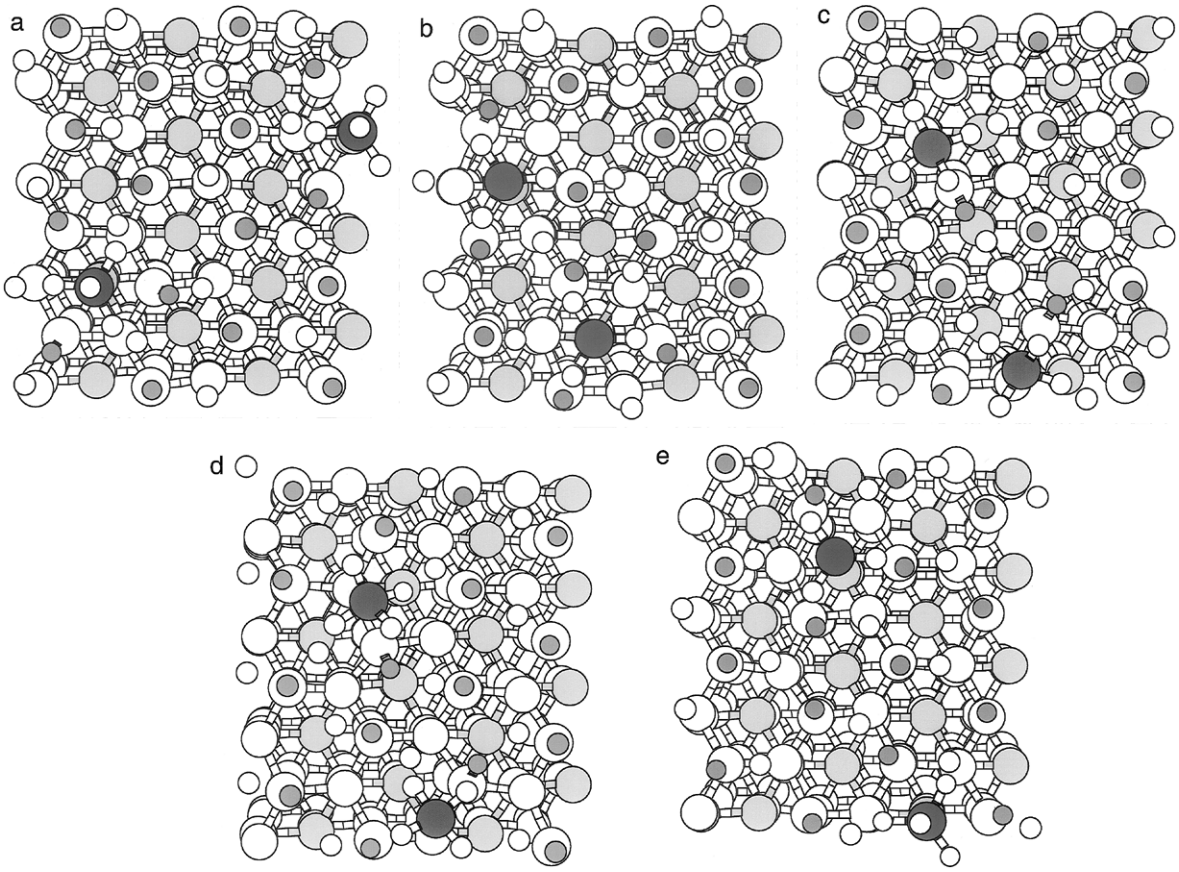

Figure 5. Still images taken from a methane system sliding simulation. These images correspond to a trajectory that yielded the data shown in Figure 4. For clarity, the carbon atoms of the upper diamond surface (Figure 1) are not shown and the color coding is as in Figure 1. The system is viewed along the [111] direction, the [11$\bar{2}$] direction is from left to right, and the [1$\bar{1}$0] direction is from bottom to top. The simulation times (sliding distance/unit cell length) are 0.050 ps (0.011), 4.2 ps (0.96), 5.8 ps (1.3), 7.0 ps (1.6), and 7.9 ps (1.8), in a, b, c, d, and e, respectively.

molecules avoid these hydrogen atoms by moving along a diagonal line to positions over second-layer carbon atoms (large white spheres, Figure 5c), which decreases the frictional force (Figure 4). The direction of the diagonal move, below or above the hydrogen atom in the sliding path, is dictated by the relative positions of the upper-surface hydrogen atoms.

Continued motion of the methane molecules in the sliding direction forces them to pass between lower-surface hydrogen atoms, which are 2.5 Å apart, and is concomitant with an increase in frictional force (Figure 4). The configuration shown in Figure 5d corresponds to a maximum in the friction trace. The upper surface is able to sweep the methane molecules through the 2.5 Å "window" between lower-surface hydrogen atoms so that the methane molecules are centered over holes in the lower diamond surface (Figure 5e). Interaction with the lower-surface hydrogen atoms is reduced; as a result, the frictional force is at a minimum. This series of motions is repeated throughout the course of the trajectory; therefore, the frictional force data shown in Figure 4 are approximately periodic.

To summarize, because of the relatively small size of the methane molecules compared to the placement of hydrogen atoms on the diamond surfaces, the methane molecules can move between the diamond surfaces without interacting significantly with the diamond-surface hydrogen atoms.[25] The strength of the interactions of these molecules with the atoms of both diamond surfaces ultimately determines the magnitude of the frictional force; therefore, this force is low when methane molecules are trapped between diamond surfaces. In addition, the spherical shape of the methane molecule limits the conformations it adopts while sliding. Thus, irrespective of load or diamond surface alignment, the motion of the methane molecules described in Figures 5a-e was observed in the majority of the simulations. This leads to friction traces that look similar regardless of the load or surface alignment. Consequently, the range of frictional force values reported for a given load is small (Figure 2).

In contrast, in the ethane and isobutane systems, the shape and periodic nature of the friction traces vary depending upon the applied load, the alignment of the surfaces, and the orientations these molecules adopt during sliding. Because ethane and isobutane are nonspherical molecules, several initial orientations of these molecules, relative to the sliding direction, are possible. For example, the orientation of the ethane molecule is defined by the angle its C−C bond makes with the sliding direction (0−180°). Confining an ethane molecule between two diamond surfaces and equilibrating the system typically leads to configurations where the C−C bond is at a diagonal (approximately 45° or 135°) to the sliding direction. Indeed, the ethane molecule began the trajectory in approximately a diagonal orientation in the majority of the simulations reported in Figure 2. (Slight variations of these orientations arise from different diamond surface alignments.) Both the ethane and isobutane molecules are too large to slide through the window between lower-surface hydrogen atoms. As a result, the molecules adopt different orientations during sliding. The sequence of orientations adopted gives rise to particular shapes in the friction trace.

The effects of molecule orientation and load on the friction trace are demonstrated in Figure 6. In this figure, the friction traces for three separate ethane simulations are shown. (At the start of the simulations the ethane molecule is oriented diagonally to the sliding direction unless otherwise indicated.) The data shown in the lower panel of this figure correspond to a low-load trajectory (0.12 nN/atom) where the diamond

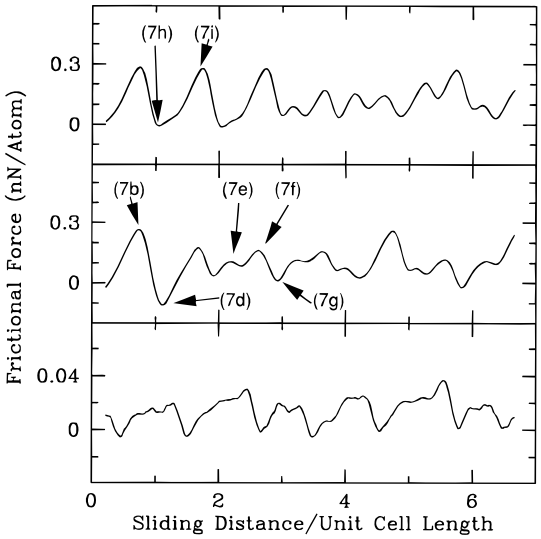

Figure 6. Frictional force as a function of sliding distance divided by unit cell length for three ethane system simulations. The average normal load and frictional force are 0.12 and 0.013 nN/atom, 0.64 and 0.090 nN/atom, and 0.63 and 0.11 nN/atom in the lower, middle, and upper panels, respectively. The data in the middle and upper panels correspond to the trajectories described in Figures 7a−g and 7h,i, respectively.

surfaces are 0.313 Å away from alignment. For this low-load trajectory, the friction trace is regular because the same series of motions of the ethane molecule is repeated throughout the course of this trajectory.

At higher loads (0.64 nN/atom), the friction trace (middle panel, Figure 6) is less regular because the ethane molecule adopts more orientations while sliding. In this trajectory, the ethane molecule is not oriented exactly along the diagonal at the start of the simulation; however, sliding quickly orients the molecule along the diagonal with the ends of the molecule located approximately over holes and second-layer carbon atoms (Figure 7a). (This motion and relative starting orientation are also observed in low-load trajectories.) Configurations of these types (Figures 7a,d) correspond to minima in the friction traces because this area on the diamond surface affords the most room for the ethane molecule and it does not interact significantly with the lower-surface hydrogen atoms.

Continued motion of the upper surface causes the leading group (further along in the sliding direction) of the ethane molecule to be pushed into the 2.5 Å window (Figure 7b). The strong interaction of the ethane molecule with the hydrogen atoms leads to a maximum in the friction trace (middle panel, Figure 6). This type of configuration is also observed at low loads. However, at low loads the ethane molecule distorts the hydrogen atoms in its path to a lesser extent. At this point in the trajectory, if the load was lower, the trailing edge of the ethane molecule could pass over the lower-surface hydrogen atom in its path. Instead, the leading end of the ethane molecule is pushed laterally in the sliding direction by an upper-surface hydrogen atom to a position over a hole in the lower surface (Figure 7c). Subsequently, the trailing end of the ethane molecule lifts away from the lower surface. The molecule pivots on its leading end and rotates about the C−C bond. The result is an ethane molecule whose C−C bond is along the opposite diagonal (Figure 7d).

Another type of motion exhibited by the ethane molecule in this trajectory is diagonal movement through the 2.5 Å window between lower-surface hydrogen atoms. This motion begins with leading and trailing ends of the ethane molecule located over a second-layer carbon atom and a hole in the lower

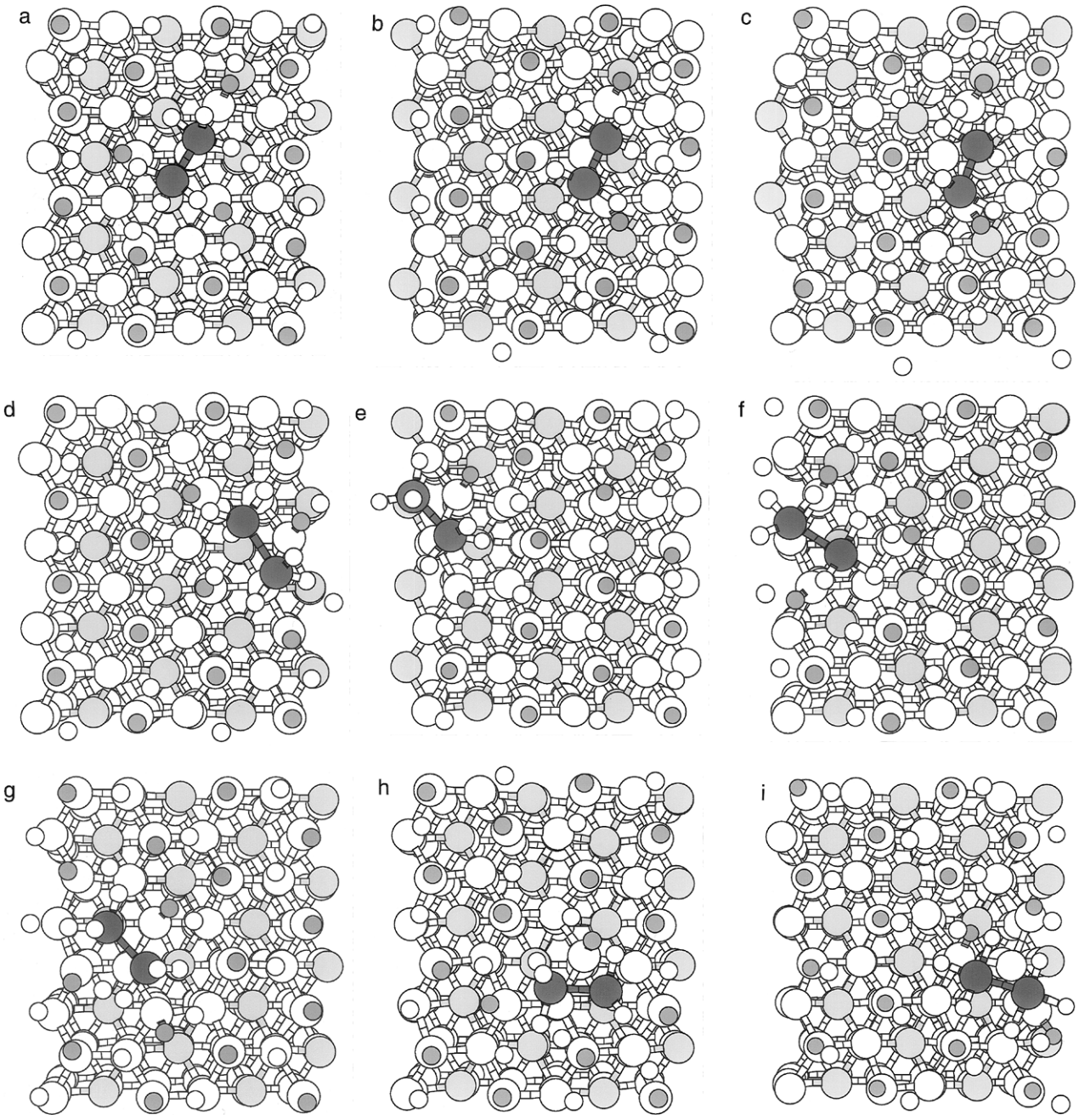

Figure 7. Still images taken from two ethane system sliding simulations. For clarity, the carbon atoms of the upper diamond surface (Figure 1) are not shown. The color coding is as in Figure 1, and the crystallographic directions are as in Figure 4. Panels a−g and h,i correspond to two different simulations. The simulation times (sliding distance/unit cell length) are 0.900 ps (0.20), 3.15 ps (0.71), 3.80 ps (0.86), 4.95 ps (1.1), 9.85 ps (2.2), 11.3 ps (2.5), 13.2 ps (3.0), 4.75 ps (1.1), and 8.25 ps (1.9) in a, b, c, d, e, f, g, h, and i, respectively.

diamond surface (Figure 7e), respectively. Motion of the upper surface causes the leading end of the molecule to slide laterally over a hole in the lower surface (Figure 7f). This motion is accompanied by a slight downward shift of the trailing end of the molecule and an increased interaction of the trailing end with a lower-surface hydrogen atom. Because of this increased interaction, this configuration corresponds to a maximum in the friction trace (middle panel, Figure 6). The ethane molecule completes its pass through this window by moving diagonally, along the line of the ethane molecule's C−C bond, to the configuration shown in Figure 7g. The leading and trailing ends of the ethane molecule are now centered over second-layer carbon atoms and holes of the lower diamond surface, respectively. Thus the frictional force is at a minimum.

Occasionally the stress on the ethane molecule caused by the sliding is large enough to break a chemical bond within the molecule. For instance, in the high-load trajectory discussed above, one end of the molecule experiences difficulty "passing by" a lower-surface hydrogen atom while a hydrogen atom from the upper surface is pushing the opposite end of the molecule. The force along the C−C bond is too great and it breaks. Due to the proximity of the nascent methyl radicals, and the absence of additional reactive species, the bond reforms. Specific tribochemical reactions and their mechanisms will be examined in detail in a future publication.[37]

On the basis of the previous analysis of sample trajectories, it is clear that the orientation adopted by the ethane molecule while sliding affects the shape of the friction trace and the magnitude of its extrema. Orientations that increase the strength of the interaction with the diamond surfaces should result in larger maxima in the friction trace. It seems likely that the strongest interaction between the diamond surfaces and the

ethane molecule would result when the ethane molecule is oriented with its C−C bond parallel to the sliding direction and in line with lower-surface hydrogen atoms. To test this hypothesis, the low- and high-load simulations discussed above were repeated with the ethane molecule parallel to the sliding direction at the start of the trajectories.

At the high load (0.63 nN/atom), the ethane molecule weaves its way between lower-surface hydrogen atoms while remaining nearly parallel to the sliding direction for the first half of the simulation (15 ps, or 3.2 unit cell distances). This is apparent from analysis of the friction trace shown in the upper panel of Figure 6. The first three minima in the friction trace correspond to configurations where the C−C bond of ethane is parallel to the sliding direction and the leading and trailing ends of the molecule are over a hole and a second-layer carbon atom, respectively (Figure 7h). Sliding the upper surface causes the leading end of the ethane molecule to interact with the lower-surface hydrogen atom directly in its path (Figure 7i). This type of interaction is responsible for the first three maxima in the friction trace. After the upper surface slides approximately three unit cell distances, the orientation of the ethane molecule changes, causing the friction trace to change. The ethane molecule is diagonally oriented, undergoing motions similar to those described earlier, until five unit cell distances, when it assumes its parallel orientation again. Because of the orientation of the C−C bond, the average frictional force for this trajectory (0.11 nN/atom) is higher than it is when the ethane molecule is diagonally oriented for the majority of the simulation (0.090 nN/atom). Similarly, at low loads, the trajectory that begins with the ethane molecule oriented parallel to the sliding direction produces a larger average frictional force (0.026 nN/atom) than the diagonally oriented trajectory (0.013 nN/atom).

Altering the alignment of the diamond surfaces, while keeping the load constant, affects the motion of the ethane molecule at both low and high loads. For example, at low loads, when the two diamond surfaces were not aligned, the ethane molecule occupies a diagonal orientation for the majority of the simulation (discussed above). In contrast, when the two diamond surfaces are aligned, the ethane molecule is pushed from a diagonal orientation (similar to Figure 7a) to a parallel orientation for parts of the simulation. Because the ethane molecule is oriented parallel to the sliding direction for part of the simulation, it is not surprising that the average frictional force is higher for this trajectory (0.021 nN/atom) than it was for the trajectory where the diamond surfaces are not aligned (0.013 nN/atom).

Thus, the range of average frictional force values obtained at a given load is dictated by the orientations the ethane molecule adopts while sliding. These orientations depend on the alignment of the diamond surfaces and the third-body-molecule's starting orientation. Configurations that lead to increased interactions with the diamond surfaces, such as the parallel orientation, lead to higher values of average frictional force for a given simulation. This accounts for the range of average frictional force values at a given load shown in Figure 2.

The shapes of the friction traces for the isobutane system simulations also depend on load, surface alignment, and orientation of the isobutane molecule (Figure 8). Of course, the orientations the molecule adopts while sliding depend on its initial orientation. For the simulations reported in Figure 2, at the start of the simulations the isobutane molecule is oriented approximately as it is in Figure 9a. (It should be noted that the starting orientation of the molecule differs slightly depending on the alignment of the diamond surfaces. When the hydrogen atoms on opposing surfaces are not aligned, there is less space for the isobutane molecule. In this case, the starting conformation is slightly distorted (Figure 9f).) In the configuration shown in Figure 9a, the methyl groups of the isobutane molecule are located above holes in the lower diamond surface and all occupy the same plane. The central carbon atom is above the plane that contains the methyl groups and is centered over a second-layer carbon atom. The hydrogen atom on the central carbon atom is pointing toward the upper diamond surface. The C−C bond between the central carbon atom and the leading methyl group is parallel to the sliding direction. Because one methyl group is pointing in the sliding direction, this molecule orientation will be referred to as the "arrow" orientation.

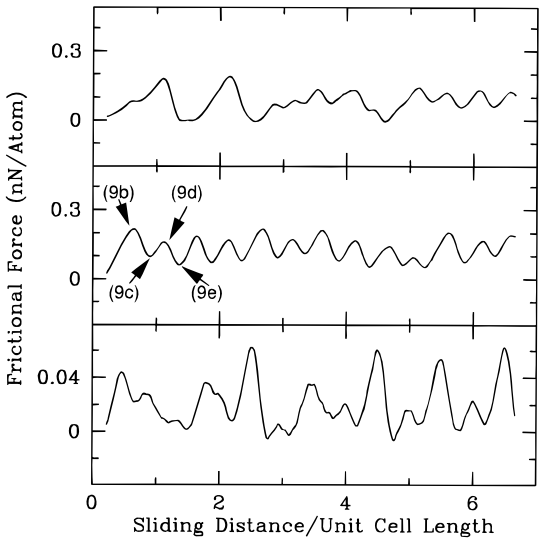

Figure 8. Frictional force as a function of sliding distance divided by unit cell length for three isobutane system simulations. Letters correspond to the configurations shown in Figure 9. The average normal load and frictional force are 0.12 and 0.020 nN/atom, 0.59 and 0.13 nN/atom, and 0.59 and 0.080 nN/atom in the lower, middle, and upper panels, respectively.

The friction traces shown in the lower and middle panels of Figure 8 correspond to isobutane system trajectories at low (0.12 nN/atom) and high (0.59 nN/atom) loads, respectively. In both trajectories, the isobutane molecule is oriented in the arrow orientation at the start of the simulation (Figure 9a) and the diamond surfaces are aligned. Both friction traces are periodic, particularly the high-load trace. At high loads, moving the upper diamond surface in the sliding direction leads to interaction of the methyl groups with lower-surface hydrogen atoms (Figure 9b). Due to the proximity of the diamond surfaces, this causes a great deal of stress in the diamond lattice and is responsible for the first maximum in the friction trace (middle panel, Figure 8). A similar configuration is responsible for the first maximum in the low-load friction trace (lower panel, Figure 8).

Because of the close proximity of the diamond surfaces, continuous sliding shifts the isobutane molecule downward along a line that is approximately 90° to the sliding direction (Figure 9c), so that the carbon atoms of the isobutane molecule are not centered above carbon atoms of the lower diamond surface. This shift is concomitant with a reduction in the frictional force (middle panel, Figure 8). While the lower-surface hydrogen atoms are no longer directly in the path of the isobutane molecule, they are in close enough proximity to inhibit the sliding. Continued motion of the upper surface brings the isobutane molecule in very close proximity to three lower-surface hydrogen atoms (Figure 9d) and results in a maximum in the friction trace (middle panel, Figure 8). Eventually, the isobutane molecule is able to pass over these lower-surface hydrogen atoms and assumes an orientation very similar to its starting configuration (Figure 9e). This type of motion is

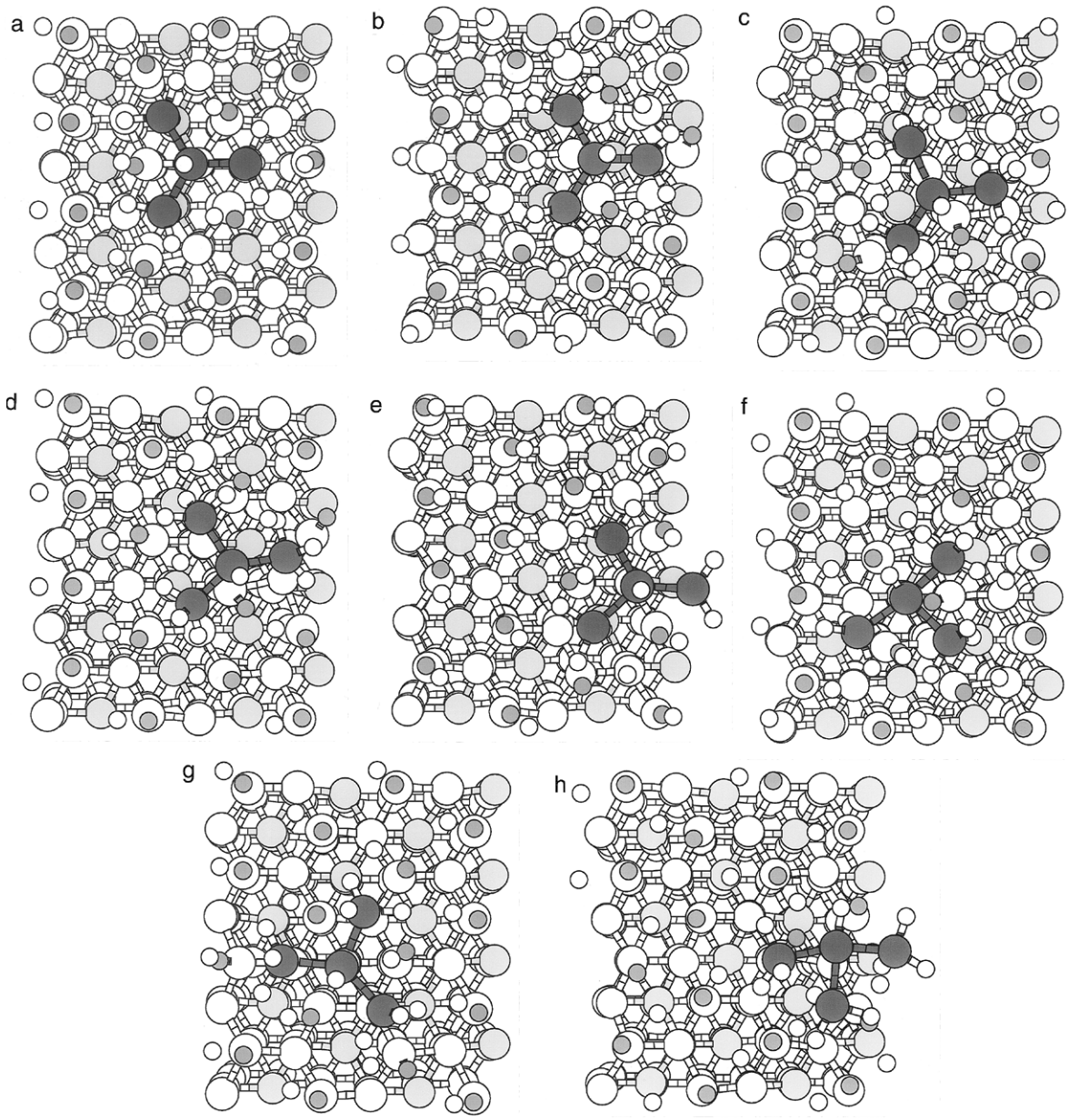

Figure 9. Still images taken from three isobutane system sliding simulations. For clarity, the carbon atoms of the upper diamond surface (Figure 1) are not shown, the color coding is as in Figure 1, and the crystallographic directions are as in Figure 4. Panels a-e, f, and g,h correspond to three different simulations. The average normal load and frictional force are 0.60 and 0.084 nN/atom for the trajectory shown in panels g,h. The simulation times (sliding distance/unit cell length) are 0.0500 ps (0.011), 2.75 ps (0.63), 3.70 ps (0.85), 4.95 ps (1.1), 5.80 ps (1.3), 0.0500 ps (0.011), 0.0500 ps (0.011), and 8.70 ps (2.0), a, b, c, d, e, f, g, and h, respectively.

repeated many times during the course of this trajectory, resulting in a periodic friction trace (Figure 8, middle panel) and an average frictional force of 0.13 nN/atom.

The low-load friction trace (lower panel, Figure 8) has differently shaped extrema than the high-load trace because different motions of the isobutane molecule are observed in this trajectory. As was indicated earlier, the motion of the isobutane molecule up to the first maximum in the friction trace is similar to the motion observed at high loads. After this, the isobutane molecule rotates to relieve the stress brought on by the interaction of the leading methyl group and the lower-surface hydrogen atom. Subsequent to the rotation, the central carbon atom is located over a lower-surface hydrogen atom. This placement of the central carbon atom is possible because the attached hydrogen atom is pointing toward the upper diamond surface. This type of configuration is usually not observed at higher loads where the proximity of the diamond surfaces causes distortion of the isobutane molecule. In addition, continued interaction with the diamond surfaces during sliding causes the isobutane molecule to occupy other orientations, some of which are observed at high loads.

As was the case for ethane, the nonspherical shape of the molecule presupposes a number of starting configurations that lead to different motions of the molecule while sliding. It seems likely that it would be most difficult to move the isobutane molecule in the sliding direction if it began the trajectory in the "sled" orientation. (In this orientation there are two leading methyl groups.) To test this hypothesis, the isobutane was placed in this orientation with the diamond surfaces aligned (Figure 9g) and a sliding simulation performed at high load. Sliding causes the molecule to encounter the lower-surface hydrogen atom in the path of the central carbon atom. The molecule distorts significantly so that its central carbon atom can pass by the hydrogen atom. This distortion (Figure 9h) worsens upon continued sliding and results in the molecule becoming stuck. The extrema in the friction trace are small

when the molecule is stuck. As a result, the average frictional force for this simulation is markedly lower (0.084 nN/atom) than it was when the molecule began the trajectory in the arrow orientation (0.13 nN/atom).

Altering the alignment of the confining surfaces changes the space available to the third-body molecule, which, in turn, affects the initial orientation and orientations adopted while sliding. In this case, altering the alignment of the surfaces causes the molecule to become stuck at various points during the course of trajectory. As before, the maxima in the friction trace are significantly smaller when the molecule is stuck (between 2.5 and 4.3 unit cell distances in the upper panel of Figure 8) than when it is free. Therefore, the average frictional force for a nonaligned trajectory is significantly less (0.080 nN/atom) than it is for the aligned trajectory (0.013 nN/atom). For the isobutane system, aligned and nonalinged orientations are usually responsible for the maximum and minimum values of average frictional force obtained at a given load (Figure 2), respectively. At low loads, the difference between aligned and nonaligned trajectories is less pronounced due to the increased spacing between the contacting surfaces.

Thus, the size of the third-body molecule relative to the spaces present on the confining surfaces plays a significant role in the friction behavior. In addition, the alignment of the confining surfaces affects the spaces present between the surfaces and therefore the orientation of the trapped molecule. Despite the fact that the ethane and isobutane molecules cause the interface layers of opposing diamond surfaces to be further apart than the methane molecules (Figure 4), the friction is larger with ethane and isobutane present because these molecules interact more with the diamond surface while sliding.

B. Friction in the Presence of a Third Body versus a Chemisorbed Group. Sliding simulations were previously carried out with hydrocarbon groups chemisorbed to one of the opposing diamond surfaces.[21] Groups with the same number of carbon atoms as the third-body molecules are compared. The systems studied are chemisorbed methyl groups versus trapped methane molecules and chemisorbed ethyl groups versus trapped ethane molecules. The average frictional force as a function of average normal load for diamond with chemisorbed methyl, ethyl, and *n*-propyl groups is shown in the upper panel of Figure 2. (These data are also averaged over diamond surface starting alignment, and the procedure is described in ref 19.) It is clear from an analysis of Figure 2 that the presence of trapped methane molecules lowers the frictional force more than the presence of chemisorbed methyl groups. In fact, the frictional force as a function of load in the presence of the chemisorbed methyl groups is approximately the same as it is in the hydrogen-terminated diamond system. Because the two methyl groups are small and bound to the diamond surface, the methyl groups interact with hydrogen atoms on the opposing diamond surface in much the same way as hydrogen atoms. As a result, at comparable loads, the interface diamond C−H layers become vibrationally excited approximately the same amount as they do in the case of pure hydrogen termination.[25] Thus, the frictional force is approximately the same.

It is interesting to note that the frictional force data as a function of interface separation are not dramatically different for the methane and the methyl-terminated systems (Figure 3). In fact, in the region between 1.5 and 2.0 Å, the curves overlap. The marked difference in the frictional force versus load data (Figure 2) arises from the higher load required to bring the methane system to the same interface separation as the methyl-terminated system.

The frictional force versus normal force data are comparable for the ethyl-terminated and the ethane systems. For both systems, these data lie on the same curve for normal forces below approximately 0.5 nN/atom. At higher loads, the frictional force for the ethyl-terminated system is slightly larger. Because the ethyl group is attached to the upper surface, it is less able to avoid interactions with atoms on the opposing surface. Thus, the mechanical interaction with the diamond is greater; therefore, the friction is higher.

As noted in a previous publication,[21] increasing the size of the chemisorbed molecule further, e.g., *n*-propyl, does not have a significant effect on the frictional force as a function of load (upper panel, Figure 2). Similarly, increasing the size of the third-body molecule from ethane to isobutane does not appear to have a significant effect on the average frictional force over the load range examined. However, it should be noted that the range of frictional force values obtained for the isobutane system is larger than the range of values obtained for the ethane system. As noted earlier, this is due, in large part, to the size of the molecule, the orientations it adopts while sliding, the spacing between atoms on the confining surfaces, and the alignment of the confining surfaces.

IV. Discussion

In this work, MD simulations have been used to examine the atomic-scale friction between two (111) faces of diamond in the presence of third-body molecules. Data obtained from these simulations were compared to previous simulations that examined the effects of chemisorbed groups on the atomic-scale friction between the (111) faces of diamond.

There are relatively few experiments that have examined the atomic-scale friction of diamond.[6,28,32,38] An AFM was used to investigate the atomic-scale friction of polished natural diamond in air using both a microfabricated Si_3N_4 tip and a single-crystal natural diamond tip.[32] In both cases, the frictional force increased as a function of load. Mate[28] used an AFM with a tungsten tip to investigate the friction of hydrogen-terminated (111) diamond in air. Again, the frictional force increased as a function of load. Comparison of these data to our simulated data is difficult because of the slight variations in the systems examined. In addition, because these experiments were conducted in air, the surfaces are probably contaminated. Despite the obvious differences between these experiments and the simulations, it is encouraging that similar trends in frictional force with load were obtained.

To date, the experiment that most closely resembles the simulation conditions is the ultrahigh-vacuum AFM experiment of Germann, *et al.*[6] In that work, the measured frictional force between a CVD diamond tip and a hydrogen-terminated diamond (111) surface was found to be independent of load. These data apparently contradict the results for the hydrogen-terminated (111) diamond surfaces in the absence of a third body. However, by comparing the shape and magnitude of the attractive force upon tip−sample retraction and approach, Germann, *et al.* concluded that the sample or tip might be covered by some physisorbed or chemisorbed species. These simulations show that chemisorbed species and molecules present between the surfaces (perhaps resembling physisorbed molecules) significantly affect the frictional force.

There are a great deal of data that examine the macroscopic friction of diamond.[27,29] These data indicate that lubricating hydrocarbon debris is formed when diamond is in sliding contact with diamond. It is not clear whether this debris originates from small fragments of diamond abraded from one surface or from the polymerization of adsorbed hydrocarbons. It is clear, however, that this debris causes significant changes in the

measured friction coefficients. Most of the recent evidence suggests that the lubricating hydrocarbon debris lowers the friction.[33] In this work, it has been shown that third-body molecules, which could perhaps model debris, reduce the friction in agreement with the data obtained from macroscopic friction experiments.

At present, there is no experimental evidence that elucidates the atomic-scale mechanism by which the debris lowers the measured friction between diamond surfaces. In contrast, due to the nature of MD simulations, the precise mechanisms by which the third-body molecules reduce friction have been identified. In the absence of third-body molecules, friction between (111) hydrogen-terminated faces of diamond arises from the mechanical interaction of hydrogen atoms on opposing surfaces during sliding. Because the third-body molecules act as a boundary layer between the diamond surfaces, the interaction between the diamond surfaces is not the major source of the friction when these molecules are present. Instead, it is the mechanical interaction of the third-body molecules with the diamond surfaces that gives rise to the friction. The magnitude of the mechanical excitation, initiated in the diamond, depends on the molecule's shape and the orientations it adopts during sliding. These orientations depend on the molecule's initial position and the relative alignment of hydrogen atoms on opposing diamond surfaces. In this work, orientations of nonspherical molecules and surface alignments that lead to high friction have been identified.

Acknowledgment. This work was supported by the U.S. Office of Naval Research (ONR) under Contract N00014−96-WR-20008. The authors would also like to thank Mark L. Elert, Christine L. Copper, and Carter T. White for many helpful discussions. Some of the figures were generated with the program XMol (XMol, version 1.3.1, Minnesota Supercomputer Center, Inc., Minneapolis, MN, 1993).

References and Notes

(1) Rabinowicz, E. *Friction and Wear*; John Wiley and Sons: New York, 1965; p 52.

(2) Bhushan, B. In *Handbook of Micro/Nanotribology*; Bhushan, B. Ed.; CRC Press: Boca Raton, FL, 1995; p 1.

(3) Krim, J. *Sci. Am.* **1996**, *October*, 74.

(4) Mate, C. M.; McClelland, G. M.; Erlandsson, R.; Chiang, S. *Phys. Rev. Lett.* **1987**, *59*, 1942.

(5) Meyer, E.; Overney, R.; Brodbeck, D.; Howald, L.; Luthi, R.; Frommer, J.; Guntherodt, H.-J. *Phys. Rev. Lett.* **1992**, *69*, 1777.

(6) Germann, G. J.; Cohen, S. R.; Neubauer, G.; McClelland, G. M.; Seki, H.; Coulman, D. *J. Appl. Phys.* **1993**, *73*, 163.

(7) Hu, J.; Xiao, X-d.; Ogletree, D. F.; Salmeron, M. *Surf. Sci.* **1995**, *327*, 358.

(8) Sheehan, P. E.; Lieber, C. M. *Science* **1996**, *272*, 1158.

(9) Israelachvilli, J. N.; McGuiggan, P. M.; Homola, A. M. *Science* **1988**, *240*, 189.

(10) Van Alsten, J.; Granick, S. *Phys. Rev. Lett.* **1991**, *16*, 33.

(11) Krim, J.; Solina, D. H.; Chiarello, R. *Phys. Rev. Lett.* **1991**, *66*, 181.

(12) Watts, E. T.; Krim, J.; Windom, A. *Phys. Rev. B* **1990**, *41*, 3466.

(13) Hirano, M.; Shinjo, K. *Phys. Rev. B* **1990**, *41*, 11837. Hirano, M.; Shinjo, K.; Kaneko, R.; Murata, R. *Phys. Rev. Lett.* **1991**, *67*, 2642.

(14) Sokoloff, J. B. *Surf. Sci.* **1984**, *144*, 267; *Phys. Rev. B* **1990**, *42*, 760.

(15) Zhong, W.; Tomanek, D. *Phys. Rev. Lett.* **1990**, *64*, 3054.

(16) McClelland, G. M.; Glosli, J. N. NATO ASI Proceedings on *Fundamentals of Friction: Macroscopic and Microscopic Processes*, Singer, I. L., Pollock, H. M., Eds.; Kluwer Academic Publishers: Dordrect, 1992; pp 405−426.

(17) Landman, U.; Luedtke, W. D. *J. Vac. Sci. Technol. B* **1991**, *9*, 414. Landman, U.; Luedtke, W. D.; Burnham, N. A.; Colton, R. J. *Science* **1990**, *248*, 454.

(18) Thompson, P. A.; Robbins, M. O. *Science* **1990**, *250*, 792. Cieplak, M.; Smith, E. D.; Robbins, M. O. *Science* **1994**, *265*, 1209.

(19) Harrison, J. A.; Brenner, D. W. *Handbook of Micro/Nanotribology*; Bhushan, B. Ed.; CRC Press: Boca Raton, FL, 1995; p 397, and references therein.

(20) Harrison, J. A.; White, C. T.; Colton, R. J.; Brenner, D. W. *Phys. Rev. B* **1992**, *46*, 9700.

(21) Harrison, J. A.; White, C. T.; Colton, R. J.; Brenner, D. W. *J. Phys. Chem.* **1993**, *97*, 6573; *Wear* **1993**, *168*, 127.

(22) Harrison, J. A.; White, C. T.; Colton, R. J.; Brenner, D. W. *Thin Solid Films* **1995**, *260*, 205.

(23) Perry, M. D.; Harrison, J. A. *J. Phys. Chem.* **1995**, *99*, 9960.

(24) Harrison, J. A.; Brenner, D. W. *J. Am. Chem. Soc.* **1994**, *116*, 10399.

(25) Perry, M. D.; Harrison, J. A. *Tribol. Lett.* **1995**, *1*, 109; *Langmuir* **1996**, *12*, 4552.

(26) Sorensen, M. R.; Jacobsen, K. W.; Stoltze, P. *Phys. Rev. B* **1996**, *53*, 2101.

(27) Tabor, D.; Field, J. E. In *The Properties of Natural and Synthetic Diamond*; Field, J. E., Ed.; Academic Press: London, 1992; p 547, and references therein.

(28) Mate, C. M. *Wear* **1993**, *168*, 17; *Surf. Coat. Technol.* **1993**, *62*, 373.

(29) Ruan, J.-A.; Bhushan, B. *J. Appl. Phys.* **1994**, *76*, 5022.

(30) Gardos, M. *Tribol. Lett.*, in press.

(31) Miyoshi, K.; Wu, R. L. C.; Garscadden, A. *Surf. Coat. Technol.* **1992**, *54/55*, 428.

(32) Bhushan, B.; Kulkarni, A. V. *Thin Solid Films* **1996**, *278*, 49.

(33) Hayward, I. P.; Field, J. E. *Proc. Inst. Mech. Eng., IMechE Conf.* **1987** *1* 205. Hayward, I. P. *Surf. Coat. Technol.* **1991**, *49*, 554, and references therein.

(34) Brenner, D. W. *Phys. Rev. B* **1990**, *42*, 9458. Brenner, D. W.; Harrison, J. A.; White, C. T.; Colton, R. J. *Thin Solid Films* **1991**, *206*, 220.

(35) Gear, C. W. *Numerical Initial Value Problems in Ordinary Differential Equations*; Prentice-Hall: Englewood Cliffs, NJ, 1971.

(36) Berendsen, H. J. C.; Postma, J. P. M.; van Gunsteren, W. F.; DiNola, A.; Haak, J. R. *J. Chem. Phys.* **1984**, *81*, 3684.

(37) Perry, M. D.; Harrison, J. A. *J. Phys. Chem.*, in preparation.

(38) van den Oetelaar, R. J. A.; Flipse, C. F. J. *Surf. Sci. Lett.*, in press.